Eur. Phys. J. A **16**, 409–414 (2003)
DOI 10.1140/epja/i2002-10110-1

THE EUROPEAN PHYSICAL JOURNAL A

Multiple Coulomb excitation of a ^{70}Ge beam and the interpretation of the 0_2^+ state as a deformed intruder

M. Sugawara[1,a], Y. Toh[2], T. Czosnyka[3], M. Oshima[2], T. Hayakawa[2], H. Kusakari[4], Y. Hatsukawa[2], J. Katakura[2], N. Shinohara[2], M. Matsuda[2], T. Morikawa[5], A. Seki[6], and F. Sakata[6]

[1] Chiba Institute of Technology, Narashino, Chiba 275-0023, Japan
[2] Japan Atomic Energy Research Institute, Tokai, Ibaraki 319-1195, Japan
[3] Heavy Ion Laboratory, Warsaw University, Warsaw PL-02097, Poland
[4] Chiba University, Inage-ku, Chiba 263-8522, Japan
[5] Kyushu University, Hakozaki, Fukuoka 812-8581, Japan
[6] Department of Mathematical Sciences, Ibaraki University, Mito, Ibaraki 310-8512, Japan

Received: 2 September 2002 / Revised version: 4 November 2002 /
Published online: 25 February 2003 –
Communicated by D. Schwalm

Abstract. Electromagnetic properties of the low-lying states in a ^{70}Ge nucleus were studied through the multiple Coulomb excitation of a ^{70}Ge beam with a ^{nat}Pb target. Relative γ-ray intensities were measured as a function of emission angle relative to the scattered projectile. Sixteen $E2$ matrix elements, including diagonal ones, for 6 low-lying states have been determined using the least-squares search code GOSIA. The expectation values $\langle Q^2 \rangle$ of 0_1^+ and 0_2^+ states in ^{70}Ge are compared with those in ^{72,74,76}Ge. Simple mixing calculations indicate that the 0_2^+ states in ^{70}Ge and ^{72}Se can be treated as deformed intruder states. It is shown that the deformed intruder becomes the ground state in ^{74}Kr. These interpretations of the 0_2^+ states in this region are compared with the potential-energy surface calculations by the Nilsson-Strutinsky model, which allow to interpret the experimental results in a qualitative way from the theoretical point of view.

PACS. 25.70.De Coulomb excitation – 21.10.Ky Electromagnetic moments – 23.20.-g Electromagnetic transitions

1 Introduction

Doubly even Se, Ge and Kr nuclei around $A \approx 80$ exhibit the shape coexistence phenomenon which arises from the competition between nuclear polarization effects associated with shell gaps at the specific nucleon number, namely $N, Z = 36$ shell gap in an oblate shape, $N, Z = 38$ one in a prolate shape and $N, Z = 40$ one near a spherical shape. In fact the excited 0^+ states corresponding to these three kinds of shapes have been observed. For example, the prolate deformed 0_2^+ state had been established in ^{72}Se [1] long time before. Recently, probably the oblate deformed 0^+ state around 500 keV was observed as an isomeric state in ^{74}Kr [2] and the nearly spherical excited 0^+ states were systematically established in ^{72,74,76}Ge [3–5].

The ^{70}Ge nucleus lies at the crossing point of two systematics, one of which is for the $Z = 32$ isotopes and the other is for the $N = 38$ isotones. Fortune and Carchidi analyzed the cross-sections for two nucleon transfer reactions and $B(E2)$ values applying the generalized two-state model to the low-lying 0^+ and 2^+ states of the ^{70,72,74,76}Ge nuclei and suggested that the two 0^+ states would interchange their character between ^{70}Ge and ^{72}Ge or between ^{72}Ge and ^{74}Ge [6,7]. It was revealed by the systematic Coulomb excitation studies recently done, that the excited 0^+ states of ^{72,74,76}Ge were mainly of spherical nature and became higher in excitation energy and purer in its character as the neutron number increased [3–5]. On the other hand, it was also shown that the prolate deformed 0_2^+ state in ^{72}Se reached the ground state at ^{74}Kr. Therefore, it is important to clarify to which systematics the 0_2^+ state in ^{70}Ge fits.

To probe the deformation of the nuclei, one of the most effective methods is to measure the Q moments and $B(E2)$ values through multiple Coulomb excitation, in which the low-lying states are excited with cross-sections directly related to the $E2$ matrix elements. Only seven $E2$ matrix elements, including 1 diagonal one, were known for the low-lying states of ^{70}Ge from the former Coulomb excitation

[a] e-mail: sugawara@pf.it-chiba.ac.jp

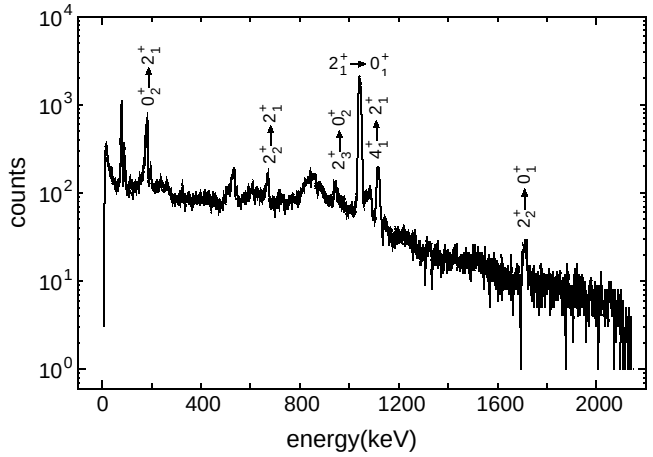

Fig. 1. The γ-ray spectrum from $^{\rm nat}$Pb(^{70}Ge,^{70}Ge$'$) at $E = 300$ MeV with Doppler correction, at a scattering angle between $\theta_{\rm lab} = 110.0^\circ$ and 160.0°.

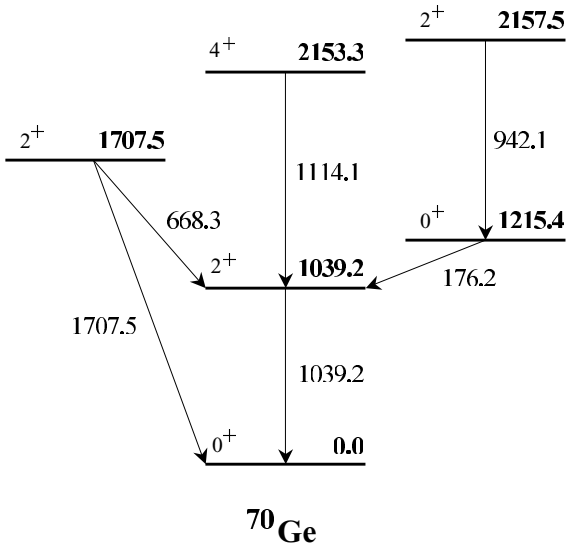

Fig. 2. Level scheme used in the analysis of ^{70}Ge and γ-transitions observed in the present experiment.

experiments [8,9] where ^{6}Li and ^{16}O beams were used. In the present work, the 16 $E2$ matrix elements, including 4 diagonal ones, connecting the 6 low-lying states were extracted from the multiple Coulomb excitation of a ^{70}Ge beam using the least-squares analysis code GOSIA.

2 Experimental procedure

The 300 MeV ^{70}Ge beam from the tandem accelerator at the Japan Atomic Energy Research Institute (JAERI) was excited on a self-supporting $^{\rm nat}$Pb target of 1.7 mg/cm^2 thickness. The γ-ray detector array, GEMINI [10], consisting of 12 HPGe detectors with BGO anti-Compton suppressor shields, was used to detect de-excitation γ-rays. The typical energy resolution was about 2.2 keV at 1.3 MeV γ-ray from ^{60}Co. The Ge detectors were placed at 32°, 58°, 90°, 122° and 148° relative to the incident beam. The scattered beam (^{70}Ge) was detected with a position-sensitive particle detector system [11] with 4 photomultiplier tubes in combination with 2 plastic and 2 Yap Ce scintillators. It covered an angular range of $30^\circ \leq \theta \leq 67^\circ$ and $106^\circ \leq \theta \leq 162^\circ$ with $\Delta\phi \approx 70^\circ$ on both sides of the beam, which corresponded to about 30% of the total solid angle. The positional resolution was 1.2 mm FWHM near the edge of the detector and 0.5 mm at the center. The information of particle position was used for Doppler correction of γ-rays from ^{70}Ge and provided the impact parameter dependence of measured γ-transitions as well. The experimental data were recorded on magnetic tapes event by event when one, at least, HPGe detector and one particle detector gave the coincident signals. About 1.6×10^8 events were collected.

In fig. 1, the γ-ray spectrum with Doppler correction is shown. The energy resolution for 1039 keV transition($2_1^+ \rightarrow 0_1^+$) was found to be 11 keV FWHM after Doppler correction. Although several non-labelled peaks were seen in fig. 1 due to random coincidences, only labelled transitions were taken into account in later analyses. The analysis of the Coulomb excitation data using the least-squares search code GOSIA was made to determine $E2$ and $M1$ matrix elements. In this analysis the angular range of the particle detector was sliced into four at the forward one and three at the backward one. Figure 2 shows the levels and transitions in ^{70}Ge observed in the present study. The six transitions of fig. 2 were taken into account in the fitting procedure. Data on the lifetimes, branching ratios and mixing ratios ($E2/M1$) from other work [12], which were listed in table 1, were included in this analysis. The GOSIA code constructs the standard χ^2 function for minimization from the measured γ yields in all experiments and scattering angle slices, as well as from the known spectroscopic data treated as γ yields, not as fixed

Table 1. Data on the lifetimes, branching ratios and mixing ratios ($E2/M1$) included in the GOSIA analysis.

Mean lifetimes (ps)	
2_1^+	1.88 ± 0.03
0_2^+	5338 ± 289
2_2^+	1.6 ± 1.4
4_1^+	1.2 ± 0.4
Branching ratios	
$2_2^+ \rightarrow 0_1^+ / 2_2^+ \rightarrow 2_1^+$	0.85 ± 0.013
$2_2^+ \rightarrow 0_2^+ / 2_2^+ \rightarrow 2_1^+$	0.046 ± 0.004
$4_1^+ \rightarrow 2_2^+ / 4_1^+ \rightarrow 2_1^+$	0.008 ± 0.002
$2_3^+ \rightarrow 0_2^+ / 2_3^+ \rightarrow 2_1^+$	0.44 ± 0.07
$2_3^+ \rightarrow 0_1^+ / 2_3^+ \rightarrow 2_1^+$	0.12 ± 0.02
$2_3^+ \rightarrow 2_2^+ / 2_3^+ \rightarrow 2_1^+$	0.033 ± 0.009
Mixing ratio ($E2/M1$)	
$2_2^+ \rightarrow 2_1^+$	-3.6 ± 1.1

Table 2. Present matrix elements $\langle I_\mathrm{i}||E2||I_\mathrm{f}\rangle$ and quadrupole moments (e · b), and previous results in ^{70}Ge.

$I_\mathrm{i} \to I_\mathrm{f}$	Present	Lecomte *et al.* [a]
$2_1^+ \to 0_1^+$	$+0.426 \pm 0.005$	$\|0.422 \pm 0.004\|$
$0_2^+ \to 2_1^+$	$+0.272 \pm 0.011$	$\|0.26 \pm 0.03\|$
$2_2^+ \to 0_1^+$	-0.0434 ± 0.0013	$\|0.037 \pm 0.014\|$
$2_2^+ \to 2_1^+$	$+0.42 \pm 0.07$	$\|0.50 \pm 0.09\|$
$2_2^+ \to 0_2^+$	$+0.25 \pm 0.02$	$\|0.13 \pm 0.06\|$
$4_1^+ \to 2_1^+$	$+0.54 \pm 0.10$	$\|0.41 \pm 0.04\|$
$4_1^+ \to 2_2^+$	-0.52 ± 0.12	—
$2_3^+ \to 0_1^+$	$+0.027 \pm 0.003$	—
$2_3^+ \to 2_1^+$	$+0.53 \pm 0.06$	—
$2_3^+ \to 0_2^+$	-0.71 ± 0.13	—
$2_3^+ \to 2_2^+$	$+0.23 \pm 0.09$	—
$2_3^+ \to 4_1^+$	$+0.86 \pm 0.12$	—
$Q_{2_1^+}$	$+0.04 \pm 0.03$	$+0.09 \pm 0.06$
$Q_{2_2^+}$	-0.07 ± 0.04	—
$Q_{4_1^+}$	$+0.22 \pm 0.05$	—
$Q_{2_3^+}$	$+0.26 \pm 0.10$	—

([a]) Coulomb excitation experiment using ^{16}O, taken from refs. [8,9]. Matrix elements are calculated from $B(E2)$ values.

values. Normalization of different data sets is done by the code so as to minimize the χ^2 values. This is possible because the excitation patterns strongly depend on different data sets, and thus absolute intensities are not needed. It was possible to derive all the $E2$ and $M1$ matrix elements connecting the 6 low-lying states of ^{70}Ge. The result of the least-squares fit reproduced the γ-ray intensities and level lifetimes well. In total, 16 $E2$ reduced matrix elements were determined including 4 diagonal ones. They were listed and compared with the previous works [8,9] in table 2. The present matrix elements are consistent with the measured values of Lecomte *et al.* derived from Coulomb excitation using ^{16}O and α beams. The uniqueness of the least-squares fitting result was confirmed by using many sets of starting values for the unknown matrix elements. The errors in table 2 include cross-correlation errors which were calculated by constructing the probability distribution in the space of fitted parameters and by requesting that the total probability is equal to the confidence limit chosen; *i.e.*, 68.3% (for details see ref. [13]). In different data sets the sensitivities to individual matrix elements are very different. Therefore, several matrix elements were determined with small uncertainties, while others, especially among weakly excited higher-lying states, could not be determined with high accuracy.

3 Results and discussion

Table 2 shows the matrix elements derived from the least-squares fit. The previous study by Lecomte *et al.* [8,9]

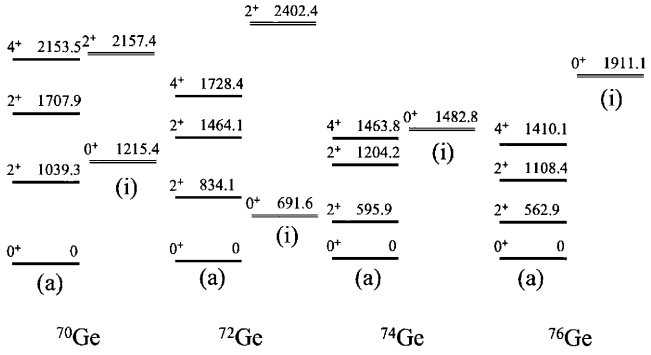

Fig. 3. Systematics of the low-lying states for $^{70\text{-}76}$Ge. Each level scheme is classified into two parts, namely the asymmetric rotor part denoted by (a) and the so-called intruder states denoted by (i).

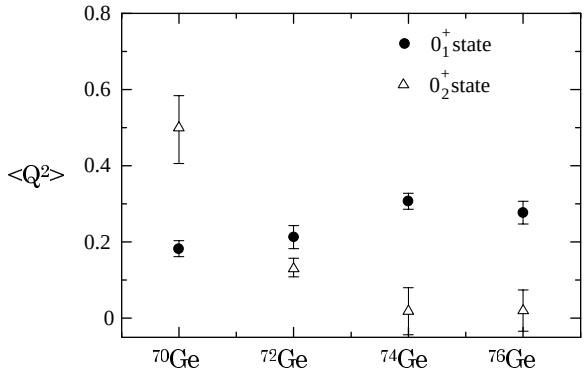

Fig. 4. Systematic change of the $\langle Q^2\rangle$ values for the 0_1^+ and 0_2^+ states from ^{70}Ge to ^{76}Ge.

left ambiguity about the sign of the interference term P_3 ($= M_{0_1 2_1} M_{0_1 2_2} M_{2_1 2_2}$, where, for example, $M_{0_1 2_1}$ stands for the reduced matrix element between the first 0^+ state and first 2^+ state). In the present study, the sign of the interference term is determined to be negative, which is opposite to the case in the heavier even-even Ge isotopes [3–5]. The present results are consistent with the previous ones [8,9], where available. The lower-lying levels of $^{70\text{-}76}$Ge are compared in fig. 3, where each level scheme is classified into two parts, namely the asymmetric rotor part (a) and the so-called intruder states (i) according to ref. [14]. At first glance one can infer that these two different structures may interchange roles between ^{70}Ge and ^{72}Ge. Following GOSIA analysis the rotational invariants, $\langle Q^2\rangle$, can be deduced using the code SIGMA [13] from the experimental $E2$ matrix elements. The centroids of $\langle Q^2\rangle$ values obtained for the two 0^+ states in $^{70\text{-}76}$Ge are presented in fig. 4. It is seen that the relative magnitudes of $\langle Q^2\rangle$ for these two 0^+ states are inverted between ^{70}Ge and ^{72}Ge, which seems to support the interpretation mentioned above. In order to further confirm this picture, we applied the simple mixing calculations including 0_1^+, 0_2^+, 2_1^+, and 2_3^+ to $^{70\text{-}76}$Ge. We assumed only 2-level mixing for both 0^+ and 2^+ states as shown in fig. 5. It is supposed that the observed states of 0_1^+, 0_2^+, 2_1^+, and 2_3^+ are composed of the "normal"(denoted by the subscript "n") and

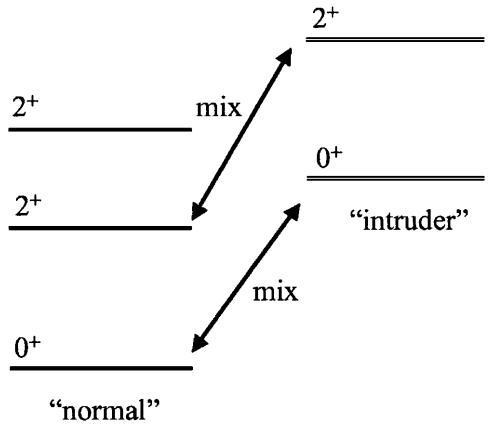

Fig. 5. Schematic picture concerning the 2-level mixing calculation.

"intruder" (denoted by the subscript "i") states as follows:

$$|0_1^+\rangle = \alpha|0_{\rm n}^+\rangle + \sqrt{1-\alpha^2}|0_{\rm i}^+\rangle\,, \quad (1)$$

$$|0_2^+\rangle = \sqrt{1-\alpha^2}|0_{\rm n}^+\rangle - \alpha|0_{\rm i}^+\rangle\,, \quad (2)$$

$$|2_1^+\rangle = \beta|2_{\rm n}^+\rangle + \sqrt{1-\beta^2}|2_{\rm i}^+\rangle\,, \quad (3)$$

$$|2_3^+\rangle = \sqrt{1-\beta^2}|2_{\rm n}^+\rangle - \beta|2_{\rm i}^+\rangle\,. \quad (4)$$

Then the $E2$ matrix elements between observed states are expressed in terms of the $E2$ matrix elements between the unperturbed states such as

$$m_{2_{\rm n}0_{\rm n}} = \langle 2_{\rm n}^+\|E2\|0_{\rm n}^+\rangle\,, \quad (5)$$

$$m_{2_{\rm i}0_{\rm i}} = \langle 2_{\rm i}^+\|E2\|0_{\rm i}^+\rangle\,, \quad (6)$$

if we neglect the $E2$ matrix elements between the "normal" and "intruder" structures because of the structural differences. The explicit formulas are as follows:

$$M_{2_10_1} = \alpha\beta m_{2_{\rm n}0_{\rm n}} + \sqrt{1-\alpha^2}\sqrt{1-\beta^2}m_{2_{\rm i}0_{\rm i}}\,, \quad (7)$$

$$M_{2_10_2} = \sqrt{1-\alpha^2}\beta m_{2_{\rm n}0_{\rm n}} - \alpha\sqrt{1-\beta^2}m_{2_{\rm i}0_{\rm i}}\,, \quad (8)$$

$$M_{2_30_1} = \alpha\sqrt{1-\beta^2}m_{2_{\rm n}0_{\rm n}} - \beta\sqrt{1-\alpha^2}m_{2_{\rm i}0_{\rm i}}\,, \quad (9)$$

$$M_{2_30_2} = \sqrt{1-\alpha^2}\sqrt{1-\beta^2}m_{2_{\rm n}0_{\rm n}} + \alpha\beta m_{2_{\rm i}0_{\rm i}}\,. \quad (10)$$

One can extract two mixing amplitudes (α, β) and two unperturbed $E2$ matrix elements($m_{2_{\rm n}0_{\rm n}}$, $m_{2_{\rm i}0_{\rm i}}$) by solving these simultaneous equations. The values for the observed matrix elements used in the calculation and the unperturbed ones obtained this way are summarized in table 3 and table 4, respectively. Now a question can be raised about the interpretation followed so far that two different structures, namely the "normal" and "intruder" states, may interchange roles between ^{70}Ge and ^{72}Ge. The large difference of the unperturbed matrix elements between ^{70}Ge and $^{72\text{-}76}$Ge, as shown in table 4, cannot convince us of such a simple picture.

We can place, however, the level structure of ^{70}Ge along another systematics of $N = 38$ isotones as shown in fig. 6, where the 0_2^+ state comes down to the ground state in ^{74}Kr. Therefore, we have applied the same simple

Table 3. The values of the observed matrix elements used in the calculation for $^{70\text{-}76}$Ge and ^{72}Se.

Nucleus	$m_{2_10_1}$ (e · b)	$m_{2_10_2}$ (e · b)	$m_{2_30_1}$ (e · b)	$m_{2_30_2}$ (e · b)
^{72}Se	0.445	0.537	0.058	$-0.772^{(a)}$
^{70}Ge	0.426	0.272	0.0273	$-0.71^{(b)}$
^{72}Ge	0.46	0.36	0.011	$0.065^{(c)}$
^{74}Ge	0.551	0.14	0.0	$0.0^{(d)}$
^{76}Ge	0.522	−0.08	0.0	$0.0^{(e)}$

(^{a}) Taken from ref. [15]. Here the 2_2^+ was adopted instead of the 2_3^+, since the 2_2^+ state was considered to be a mixture of the "normal" and "intruder" structures [15]. The signs of matrix elements were adopted in accordance with those in ^{70}Ge.
(^{b}) This work.
(^{c}) Taken from ref. [3]. Although only upper limits to the absolute values were known for $m_{2_30_1}$ and $m_{2_30_2}$, the central values assuming the positive sign were used here.
(^{d}) Taken from ref. [4]. Since the 2_3^+ state was not observed in ref. [4], the values for $m_{2_30_1}$ and $m_{2_30_2}$ were assumed to be 0.
(^{e}) Taken from ref. [5]. Since the 2_3^+ state was not observed in ref. [5], the values for $m_{2_30_1}$ and $m_{2_30_2}$ were assumed to be 0.

Table 4. Results of the simple mixing calculation for $^{70\text{-}76}$Ge and ^{72}Se.

Nucleus	α	β	$m_{2_{\rm n}0_{\rm n}}$ (e · b)	$m_{2_{\rm i}0_{\rm i}}$ (e · b)
^{72}Se	−0.967	0.756	−0.387	0.967
^{70}Ge	−0.974	0.885	−0.400	0.775
^{72}Ge	0.784	0.996	0.586	0.044
^{74}Ge	0.969	1.0	0.569	0.0
^{76}Ge	−0.988	−1.0	0.528	0.0

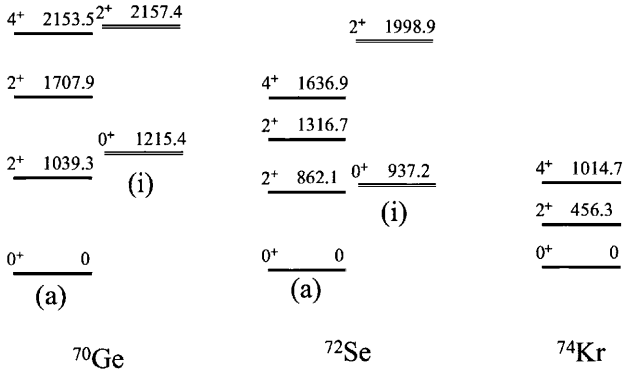

Fig. 6. Systematics of the low-lying states for $N = 38$ isotones. The same classification scheme as in fig. 3 is used.

mixing calculation to ^{72}Se which is the isotone of ^{70}Ge and have added the result to table 4. Here, one can recognize the close similarity in both the mixing amplitudes and the unperturbed matrix elements between ^{70}Ge and ^{72}Se. It is then natural to interpret the 0_2^+ state in ^{70}Ge as a deformed intruder like the case in ^{72}Se differently from the heavier even-even Ge isotopes. It can be said that there is a structural discontinuity between ^{70}Ge and ^{72}Ge. At

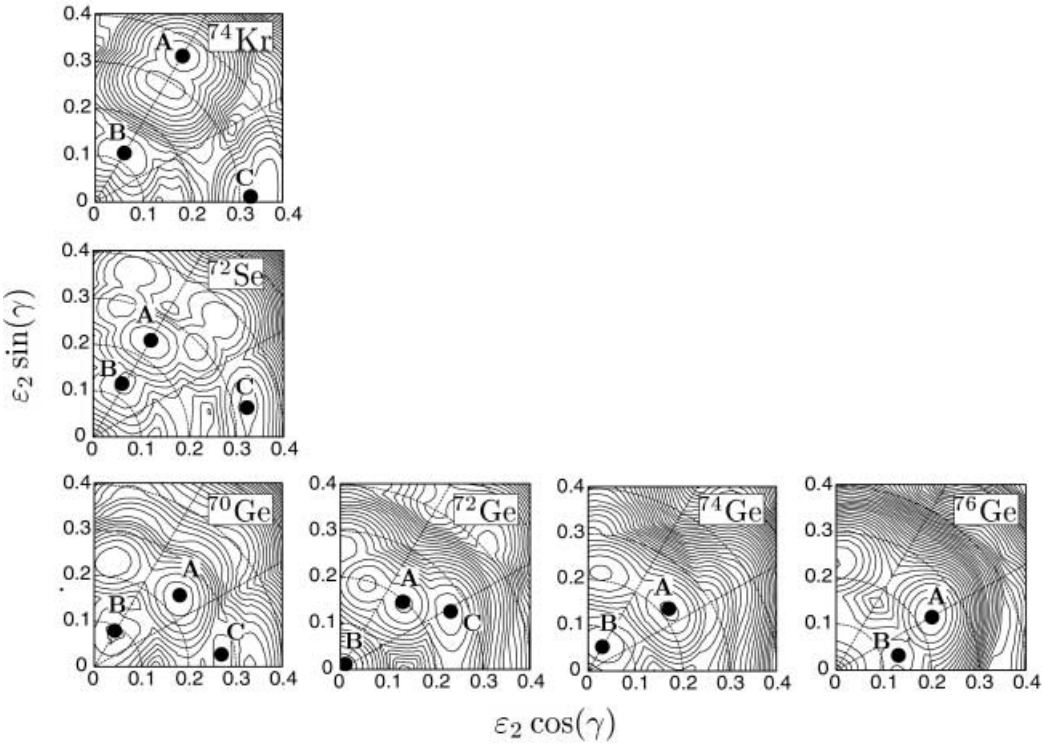

Fig. 7. Potential-energy surfaces of ^{74}Kr, ^{72}Se and $^{70\text{-}76}$Ge calculated with the Nilsson-Strutinsky model. The energy difference between contour lines is 250 keV. Two dashed lines from the origin indicate $\gamma = 30^\circ$ (lower one) and $\gamma = 60^\circ$ (upper one). Three local minima with different deformations are pointed and marked by A, B and C (respectively, A: axial asymmetric or near oblate, B: near spherical, C: near prolate) as discussed above.

last it is worth pointing out that the unperturbed $E2$ matrix elements $m_{2_i 0_i}$ within the deformed intruder structure for ^{70}Ge and ^{72}Se vary smoothly and continue to the $E2$ matrix element between 0_1^+ and 2_1^+ in ^{74}Kr, where the deformed intruder state comes down to the ground state, specifically from 0.775 in ^{70}Ge and 0.967 in ^{72}Se to 0.939 in ^{74}Kr [12].

To get the theoretical implications to the interpretations of the 0_2^+ states in this region mentioned above, we performed the potential-energy surface calculations using the Nilsson-Strutinsky model [16,17]. The strength parameters of $\boldsymbol{\ell} \cdot \boldsymbol{s}$ and $\boldsymbol{\ell}^2$ forces were taken from ref. [18] in the Nilsson potential. The frequency parameter of the spherical harmonic-oscillator potential for proton or neutron, $\omega_0(\varepsilon_2 = 0)_{\mathrm{p/n}}$, was taken as

$$\hbar\omega_0(\varepsilon_2 = 0)_{\mathrm{p/n}} = \frac{41}{A^{1/3}}\left(1 \pm \frac{N-Z}{3A}\right) \quad \mathrm{MeV},$$

respectively. For the parameters of the liquid-drop part, that is, the Weizsacker-Bethe mass formula, the following values were adopted according to ref. [19]:

$$a_v = 15.4941 \quad \mathrm{MeV}\,,$$
$$a_s = 17.9439 \quad \mathrm{MeV}\,,$$
$$a_c = 0.70531 \quad \mathrm{MeV}\,,$$
$$\kappa_v = \kappa_s = 1.7826\,,$$
$$d = 0.546 \quad \mathrm{fm}\,,$$
$$R_c = 1.2249A^{1/3} \quad \mathrm{fm}\,.$$

The results of the Nilsson-Strutinsky calculations were shown as the contour plots of potential-energy surfaces for ^{74}Kr, ^{72}Se and $^{70\text{-}76}$Ge, which were arranged according to Z and N, in fig. 7. Here we paid attention to three local minima with different deformations, which were pointed and named A, B and C (A: axial asymmetric or near oblate, B: near spherical, C: near prolate). If we trace figures from ^{76}Ge to ^{74}Kr, one can recognize that the minimum A (axial asymmetric) in ^{74,76}Ge bifurcates and develops to A and C (near oblate and near prolate) in ^{74}Kr, ^{72}Se and ^{70,72}Ge. For further information, relative energies of these local minima were shown in fig. 8. Although the minimum C is neither the second 0^+ state in ^{70}Ge nor the ground state in ^{74}Kr, the systematic features that the minimum C comes down to compete with B in the left part of the figure look quite supportive in a qualitative way to our interpretations of the 0_2^+ states in this mass region.

4 Conclusion

The Coulomb excitation experiment of the ^{70}Ge beam was performed with a $^{\mathrm{nat}}$Pb target. Sixteen $E2$ matrix elements including 4 diagonal ones for 6 low-lying states have been determined using the least-squares search code GOSIA. The present results turned out to be consistent

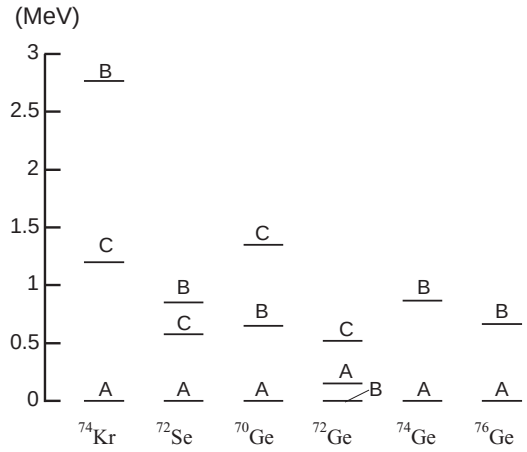

Fig. 8. Relative energies of the local minima A, B and C in fig. 7 for ^{74}Kr, ^{72}Se and $^{70\text{-}76}$Ge.

with the previous ones, where available. The rotational invariants $\langle Q^2 \rangle$ of the two 0^+ states were compared for $^{70\text{-}76}$Ge. We have made the 2-level mixing calculations including the $0^+_{1,2}$ and $2^+_{1,3}$ states and obtained the mixing amplitudes of the "normal" and "intruder" structures and the unperturbed matrix elements. Although at first it seems like the "normal" and "spherical intruder" structures may interchange roles between ^{70}Ge and ^{72}Ge from the level systematics and the comparison of the $\langle Q^2 \rangle$ values, the results of the 2-level mixing calculation suggest that it is more appropriate to interpret the 0^+_2 state in ^{70}Ge as a "deformed intruder" state like that in ^{72}Se differently from the heavier Ge isotopes. To get the theoretical suggestion to this interpretation, the potential-energy surface calculation was made using the Nilsson-Strutinsky model. It was indicated that the systematic features of these calculations were quite supportive in a qualitative way to our interpretations of the 0^+_2 states in this mass region.

We would like to express gratitude to the crew of the JAERI tandem accelerator for providing a ^{70}Ge beam.

References

1. J.H. Hamilton, A.V. Ramayya, W.T. Pinkston, R.M. Ronningen, G. Garcia-Bermudez, H.K. Carter, R.L. Robinson, H.J. Kim, R.O. Sayer, Phys. Rev. Lett. **32**, 239 (1974).
2. C. Chandler, P.H. Regan, C.J. Pearson, B. Blank, A.M. Bruce, W.N. Catford, N. Curtis, S. Czajkowski, W. Gelletly, R. Grzywacz, Z. Janas, M. Lewitowicz, C. Marchand, N.A. Orr, R.D. Page, A. Petrovici, A.T. Reed, M.G. Saint-Laurent, S.M. Vincent, R. Wadsworth, D.D. Warner, J.S. Winfield, Phys. Rev. C **56**, 2924 (1997).
3. B. Kotliński, T. Czosnyka, D. Cline, J. Srebrny, C.Y. Wu, A. Bäcklin, L. Hasselgren, L. Westerberg, C. Baktash, S.G. Steadman, Nucl. Phys. A **519**, 646 (1990).
4. Y. Toh, T. Czosnyka, M. Oshima, T. Hayakawa, H. Kusakari, M. Sugawara, Y. Hatsukawa, J. Katakura, N. Shinohara, M. Matsuda, Eur. Phys. J. A **9**, 353 (2000).
5. Y. Toh, T. Czosnyka, M. Oshima, T. Hayakawa, H. Kusakari, M. Sugawara, A. Osa, M. Koizumi, Y. Hatsukawa, J. Katakura, N. Shinohara, M. Matsuda, J. Phys. G **27**, 1475 (2001).
6. M. Carchidi, H.T. Fortune, G.S.F. Stephans, L.C. Bland, Phys. Rev. C **30**, 1293 (1984).
7. H.T. Fortune, M. Carchidi, Phys. Rev. C **36**, 2584 (1987).
8. R. Lecomte, M. Irshad, S. Landsberger, P. Paradis, S. Monaro, Phys. Rev. C **22**, 1530 (1980).
9. R. Lecomte, M. Irshad, S. Landsberger, G. Kajrys, P. Paradis, S. Monaro, Phys. Rev. C **22**, 2420 (1980).
10. K. Furuno, M. Oshima, T. Komatsubara, K. Furutaka, T. Hayakawa, M. Kidera, Y. Hatsukawa, M. Matsuda, S. Mitarai, T. Shizuma, T. Saitoh, N. Hashimoto, H. Kusakari, M. Sugawara, T. Morikawa, Nucl. Instrum. Methods Phys. Res. A **421**, 211 (1999).
11. Y. Toh, M. Oshima, T. Hayakawa, Y. Hatsukawa, J. Katakura, M. Matsuda, H. Iimura, H. Kusakari, D. Nishimiya, M. Sugawara, Y.H. Zhang, Rev. Sci. Instrum. **73**, 47 (2002).
12. National Nuclear Data Center, Brookhaven National Laboratory.
13. T. Czosnyka, D. Cline, L. Hasselgren, C.Y. Wu, Nucl. Phys. A **458**, 123 (1986).
14. W. -T. Chou, D.S. Brenner, R.F. Casten, R.L. Gill, Phys. Rev. C **47**, 157 (1993).
15. J.H. Hamilton, H.L. Crowell, R.L. Robinson, A.V. Ramayya, W.E. Collins, R.M. Ronningen, V. Maruhn-Rezwani, J.A. Maruhn, N.C. Singhal, H.J. Kim, R.O. Sayer, T. Magee, L.C. Whitlock, Phys. Rev. Lett. **36**, 340 (1976).
16. S.G. Nilsson, I. Ragnarsson, *Nuclear Structure* (Cambridge University Press, Cambridge, 1995).
17. K. Langanke, J.A. Maruhn, S.E. Koonin, *Computational Nuclear Physics 1* (Springer-Verlag, New York, 1991).
18. T. Bengtsson, I. Ragnarsson, Nucl. Phys. A **436**, 14 (1985).
19. W. Nazarewicz, P. Rozmej, Nucl. Phys A **369**, 396 (1981).